Check for updates

RESEARCH ARTICLE

REVISED Mission-based optimal morphing parameters for rotors with combined chord and twist morphing

[version 2; peer review: 2 approved]

Rohin Kumar Majeti[1], Stephan Benz[2]

[1]German Aerospace Center (DLR), Braunschweig, Germany
[2]Technical University of Braunschweig, Braunschweig, Germany

v2 **First published:** 12 Oct 2021, **1**:121
https://doi.org/10.12688/openreseurope.14060.1
Latest published: 07 Jun 2022, **1**:121
https://doi.org/10.12688/openreseurope.14060.2

Abstract

Background: The rotor blades with fixed geometry in today's helicopters do not give the best performance throughout the duration of any mission. However, low-speed and high-speed flights have different geometrical requirements for the shape of the most efficient rotor blades. With advancements in morphing technologies, these can be applied to change the shape of the blades between different flight regimes.
Methods: Two different helicopter rotor morphing concepts – namely, the linearly variable chord extension and the torque-tube based twist - under the framework of the European project SABRE were investigated for their optimal geometric parameters using a Particle Swarm Optimization (PSO) algorithm. Since the morphing parameters were dependent on the mission profile, three different missions representing typical helicopter applications were chosen. The optimization problem was posed both as single objective (power) and as multi-objective (power, tip elastic torsion and vibratory hub load). Based on the insights drawn from these investigations, a rotor was set up including both morphing concepts in a single blade.
Results: The rotor with combined chord and twist morphing was shown to give performance improvement of 6.8% over the baseline blade for a whole mission while keeping the penalty on the elastic torsion and vibration of the rotor to a minimum. The performance improvement was higher at 13% for hover and low speed flight of μ = 0.14.
Conclusions: Chord and twist are both important parameters determining the efficiency of a rotor blade. Since they have non-overlapping requirements, combining the two morphing concepts into a single blade can yield higher performance than the individual ones.

Keywords

SABRE, Morphing, Helicopter rotor, Particle swarm optimization, Optimization

Open Peer Review

Approval Status ✓ ✓

	1	2
version 2 (revision) 07 Jun 2022	✓ view	✓ view
version 1 12 Oct 2021	? view	✗ view

1. **Wen Zhong Shen**, Yangzhou University, Yangzhou, China

2. **Manfred Hajek**, Technical University of Munich, Munich, Germany

Any reports and responses or comments on the article can be found at the end of the article.



This article is included in the Horizon 2020 gateway.



This article is included in the Vehicle Engineering collection.

Corresponding author: Rohin Kumar Majeti (kumar.rohin@gmail.com)

Author roles: Majeti RK: Conceptualization, Data Curation, Formal Analysis, Investigation, Methodology, Resources, Software, Supervision, Validation, Visualization, Writing – Original Draft Preparation; **Benz S**: Data Curation, Formal Analysis, Software, Visualization

Competing interests: No competing interests were disclosed.

Grant information: This research was financially supported by the European Union's Horizon 2020 research and innovation programme under the grant agreement No 723491 (Shape Adaptive Blade for Rotorcraft Efficiency [SABRE])
The funders had no role in study design, data collection and analysis, decision to publish, or preparation of the manuscript.

Copyright: © 2022 Majeti RK and Benz S. This is an open access article distributed under the terms of the Creative Commons Attribution License, which permits unrestricted use, distribution, and reproduction in any medium, provided the original work is properly cited.

How to cite this article: Majeti RK and Benz S. **Mission-based optimal morphing parameters for rotors with combined chord and twist morphing [version 2; peer review: 2 approved]** Open Research Europe 2022, **1**:121
https://doi.org/10.12688/openreseurope.14060.2

First published: 12 Oct 2021, **1**:121 https://doi.org/10.12688/openreseurope.14060.1

REVISED **Amendments from Version 1**

The authors are grateful to the reviewers for their constructive comments and suggestions. The following changes have been made to the text in the revised version:

- Literature review has been expanded to highlight what is lacking in the current state-of-the-art and the contribution of the current work.

- Properties of the baseline rotor blade have been included in the form of figures and important geometrical values have been added.

- More details of surrogate models have been added.

- The section on Rotor comprehensive analysis aerodynamics has been updated with more details of CFD analysis and unsteady aerodynamic modeling added.

- Figures in the results section have been updated. Figures for variation of the total mission objective of the chord morphing case for different scenarios have been grouped together. Important data points in the figures for the variation of the total mission objective of twist morphing for different scenarios have been grouped together.

- Reasons for the observed decrease in power savings with velocity for the chord morphing case have been spelled out.

- More light has been shed on the observed large reduction in the Fz4K for the combined morphing case at high velocity

Any further responses from the reviewers can be found at the end of the article

Plain language summary

In order to have the best performance, helicopters require their rotor blades to have different shapes in hover and at various flight speeds. However, due to manufacturing constraints and technology limitations, most helicopter rotor blades have rectangular shapes as a compromise. As technology progresses, it is possible today to have morphing blades which change shape with change in flight speed. Using an optimization algorithm called particle swarm optimization (PSO), the current work aims to find the best possible rotor blade shape during the course of a mission. A mission, usually, has all flight regimes – hover, low-speed and high-speed – in different proportions. The morphing is assumed to take place in a quasi-static manner when there is a transition of flight regime (speed). Within any flight regime, the shape of the blade remains unchanged. Two different morphing concepts - one involving linearly variable chord along the length of the blade and another with varying twist along the length of the blade, are investigated. Based on the insights drawn from this study, a blade having varying chord (width of rotor blade) in the inboard sections of the blade and varying twist (angle that the chord line at any section makes with the chord line at the root section) in the outboard sections of the blade was set up. This blade with combined morphing characteristics was shown to have better performance than the baseline blade.

Introduction[1]

It is a challenge to design a helicopter's main rotor to operate efficiently through all stages of a mission while maintaining its vibration and stress limits. The fixed geometry rotor in current helicopters is a compromise between various competing needs of different flight regimes in a mission. Rather, a morphing rotor capable of changing its geometry can handle these competing objectives better. With the primary objective of reducing helicopter emissions, several rotor morphing concepts are being researched within the European project Shape Adaptive Blades for Rotorcraft Efficiency, SABRE www.sabreproject.eu[1]. Within SABRE, the German Aerospace Center (DLR) is responsible for the variable chord extension concept[2] while twist morphing[3,4] and camber morphing[5] are the focus of research for a few other partners. Morphing was achieved in these cases through the use of innovative actuation mechanisms[6]. In general, morphing can be actuated either quasi-statically (as a function of flight condition) or dynamically (as a function of azimuth)[7].

Optimization techniques have been used in helicopter rotor design for more than three decades now for aerodynamic[8] as well as structural[9] objectives. These techniques reduce the workload of obtaining the optimum design from the designer. Since analysis and design of the helicopter rotor is multidisciplinary in nature, over the years, researchers have also performed optimization taking into account the couplings between aerodynamics, dynamics and structures[10–12]. These optimization procedures have dealt with a large number of design variables and multiple objectives like performance, vibration, noise and weight being met simultaneously.

A large body of work on optimization of locations of active trailing-edge flaps on helicopter blades for vibration reduction, reduction of dynamic twist and performance enhancement using surrogate-based approaches like Neural Networks is available in literature[13–15]. A similar study as in Ref. 15 was undertaken for active twist rotors in Ref. 16. There is, however, a lack of optimization studies on chord morphing based vibration reduction or performance improvement approaches. In Ref. 17, a gradient-based aerostructural optimization approach that simultaneously optimizes the mission and design of the morphing wing to reduce the fuel burn required to complete a certain mission was carried out, albeit for a fixed-wing aircraft. Designing the wing, morphing inputs and mission trajectory simultaneously gives maximal benefit. There is a lack of such mission-based optimization approaches for morphing helicopter rotors in literature.

Several strategies for optimization have been discussed at length in 18. Many of these strategies require gradient information to determine the direction of the global optimum. However, these strategies are met with problems when there are multiple local minima. Evolutionary methods of optimization like genetic algorithm, on the other hand, require only the functional values and not the gradients. Particle swarm optimization (PSO) is an evolutionary algorithm based on the behavior of a colony of living organisms such as a flock of birds[19]. The method does not require gradients and can find global optima based on randomized start points and the knowledge of the current global and personal minima through its iterative, population-based character. This makes it suitable for running

[1]Presented at the 8th Asian/Australian Rotorcraft Forum, Ankara, Turkey, Oct. 30 - Nov. 2, 2019.

iterative and computationally expensive numeric programs. PSO has recently gained popularity for use in helicopter rotor design[20–22]. The geometry of a morphed rotor, whether morphed in chord or twist, is described by a set of additional parameters. Since requirements for rotor design, like performance or vibrations, are different for hover and for forward flight, the geometry of the morphed rotor changes throughout any particular mission. Thus, morphing parameters are mission-dependent, and also change during the course of the mission. In the current work, the optimal geometrical parameters for a morphing rotor were determined for each flight regime and presented using PSO combined with an aerostructural analysis. Different standard missions were investigated for their effect on the morphing parameters. Each mission has predefined flight regimes (velocities) with set durations. The morphing mechanism is assumed to be quasi-static in nature, which means that the blade shape is fixed in each flight regime and the morphing to a different shape takes place only during the transition between flight regimes. The combined effect of the investigated systems in a single blade was also looked into. The focus of the current study is on the optimization study rather than on the details of the morphing mechanism.

Methods

Morphing concepts

Two morphing concepts will be considered in this paper – the linearly variable chord-extension morphing concept of DLR[2] and the twist morphing using shape memory alloy (SMA) torque-tubes concept of CIRA Italy[4].

It is known that for the so-called "optimum hovering rotor", the blade chord and the twist distribution of the blade both vary hyperbolically with span length[23] as in Figure 1. Based on this principle, in the linearly variable chord-extension morphing concept, the trailing edge is hinged out as shown in Figure 2. In addition to the chord-extension, another feature was also included in the morphing rotor. This involved deflecting the extended chord in a similar manner as would be done with a trailing-edge flap, thereby introducing an effective twist (Figure 3). Thus, in this concept, the blade chord as well

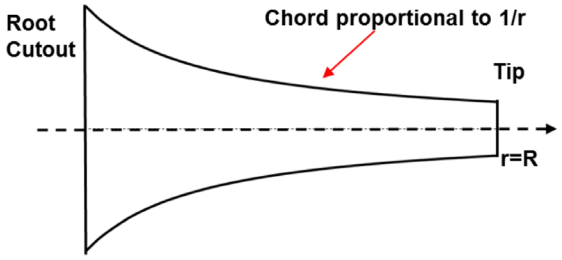


Figure 1. Top view of optimum hovering rotor blade.

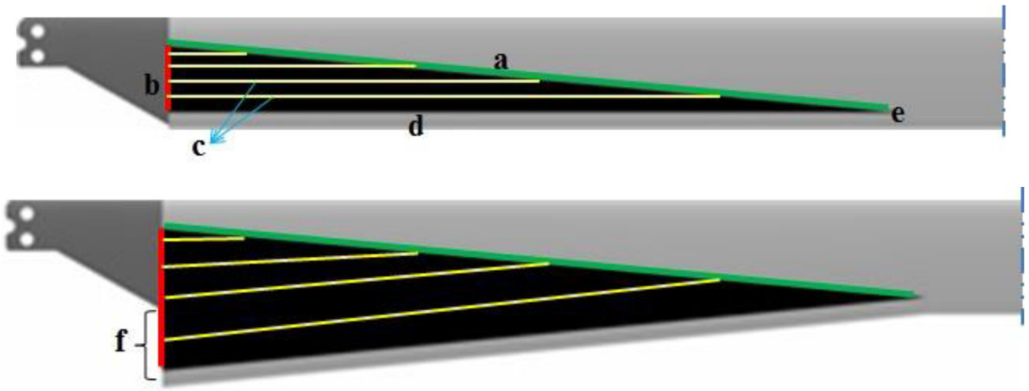


Figure 2. Top view of unmorphed rotor blade (top) and the fully extended rotor blade with a) auxiliary spar (green), b) guidance system (red), c) web stiffeners, d) rear spar, e) hinge, f) maximum chord-extension (Δ_c).

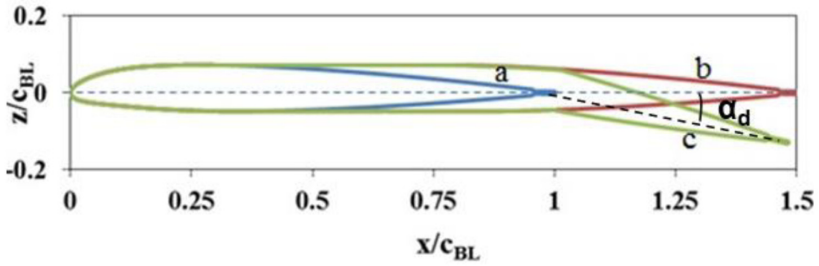


Figure 3. NACA23012tab airfoil with chord-extension and deflection. a) Baseline airfoil, b) with 50% chord-extension, c) with 50% chord-extension and deflection.

as the blade twist taper down from near the inboard region to a constant value from some point (hinge) in the outboard region. The location of this hinge is a variable to be determined based on the required desirable characteristics and performance of the blade.

The structural arrangement for the linearly variable chord-extension morphing is described as follows referring to Figure 2. A rear spar (d) is located in the trailing edge and can be swept back around a hinge (e) which is located at a desired blade radius. At the innermost radial location of the aerodynamic section (at 22% blade radius) this spar is actuated perpendicular to the radial direction by an actuator (b). It is to be noted that the term 'maximum chord-extension' refers to the chord-extension at this location.

In the torque-tube twist concept, a pre-twisted SMA tube with flanges on either end is inserted into the blade section by removing foam material and connected through the flanges to the leading-edge C-Spar (Figure 4). By heating the tube to varying degrees when required, the desired twist (upto Δ_{max} = -16deg) may be transmitted to the blade.

Morphing parameters. As mentioned earlier, the geometry of the morphed rotor can be described by morphing parameters. The set of morphing parameters for the two morphing concepts in consideration are given in Table 1. It is to be noted that for a particular mission, parameter *i1* is fixed for the chord-morphing case while parameters *i2* and *i3* are expected to be varied during the course of the mission depending on the objectives. Similarly, for the twist morphing case, parameters *i1* and *i2* are fixed for a particular mission while parameter *i3* is expected to be varied over the course of the mission.

Mission description

Helicopters are used for a variety of missions because of their hovering and loitering capacity. Recognizing that the optimum total power requirement is mission dependent, three different mission profiles, namely a military mission, a search and rescue (SAR) mission and a regular transport mission have been selected for this work[24,25]. These missions give an overview of typical helicopter applications. The mission profiles are shown in Figure 5. Details of each mission have been taken from said references. Each leg of a specific mission has been given a weightage proportionate to its duration with respect to the overall mission duration. The weightages (w_{vi}) are shown in Table 2. Mission 1 has longer hover and low velocity phases compared to the high velocity phase while mission 3 has shorter hover phase compared to the high velocity phase. Mission 2 has a uniformly distributed velocity profile. The altitude variations during the course of the missions are not considered large enough to cause much variations in air density. Hence, for all practical purposes, air density is considered to be constant throughout any mission. The absolute altitudes of flight are not relevant for the relative power analysis of morphing configurations as much as the duration of each leg of the mission.

Optimization problem definition

The linearly variable chord morphing and twist morphing concepts have been individually shown to be effective in improving the overall performance of the rotor[2,4]. But this

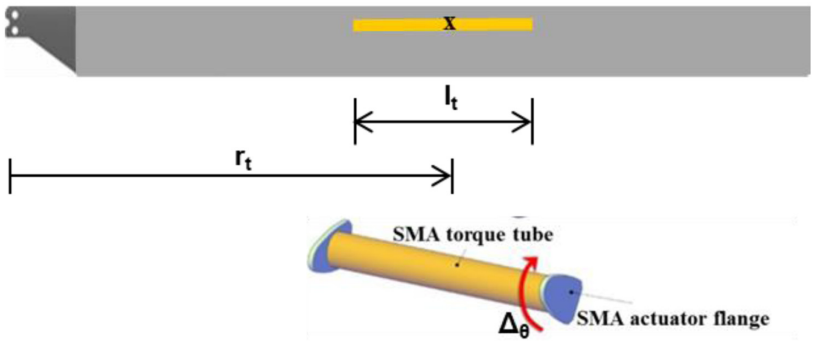


Figure 4. SMA driven twist concept[3].

Table 1. Morphing parameters.

Parameter	Chord-morphing	Twist-morphing
i1	Non-dimensional radial location of hinge, r_h, wrt R	Non-dimensional radial location of torque-tube center, r_t, wrt R
i2	Non-dimensional maximum chord extension, Δ_c as % of C	Non-dimensional torque-tube length, l_t, wrt R
i3	Chord deflection, α_d	Percent twist of torque-tube, Δ_θ

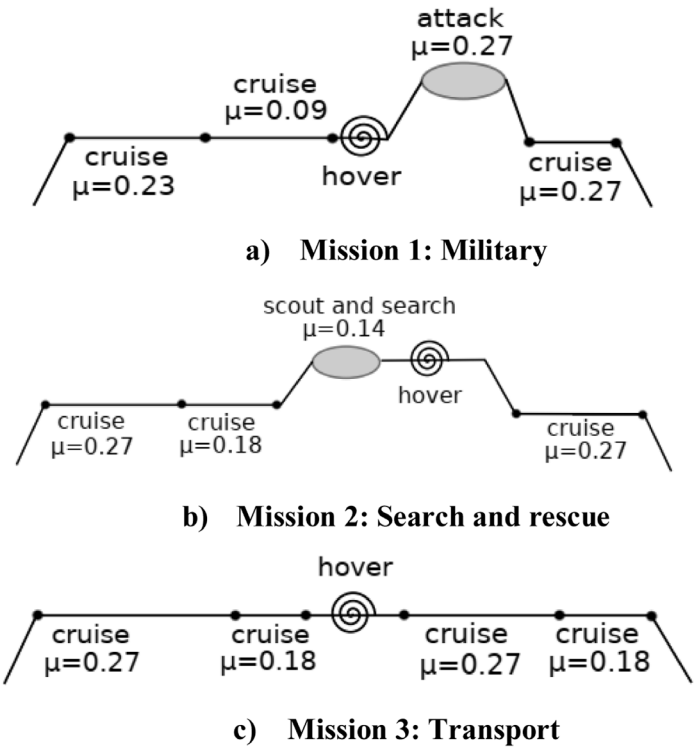


Figure 5. Selected mission profiles.

Table 2a. Mission 1 profile.

Velocity (m/s)	Advance ratio μ	Duration (s)	w_{vi} %
0	0.0	1500	25
20	0.09	1796	31
50	0.23	718	13
60	0.27	1800	31

Table 2b. Mission 2 profile.

Velocity (m/s)	Advance ratio μ	Duration (s)	w_{vi} %
0	0.0	120	12
30	0.14	250	24
40	0.18	120	12
60	0.27	530	52

Table 2c. Mission 3 profile.

Velocity (m/s)	Advance ratio μ	Duration (s)	w_{vi} %
0	0.0	60	7
40	0.18	240	29
60	0.27	530	64

improvement in performance came at the cost of a high elastic twist for both the concepts. The question arises, whether combining the two concepts results in synergizing their benefits, giving rise to better performance with minimum penalty or even reduction of the loads and vibrations. The combined morphing poser, by virtue of the large design space of possible morphing parameter values, lends itself to an optimization study. However, prior to combining the two morphing concepts, a detailed optimization study of the individual concepts for different missions is desired. The optimization algorithm chosen for the current work was the PSO due to its lesser function evaluations compared to other evolutionary algorithms. Details of the PSO implementation used in this work are given in 22, a brief summary of which is given in the sub-section below. The PSO algorithm is combined with S4, the in-house comprehensive analysis code at DLR[26,27], which analyses helicopter rotors in hover and forward flight. S4 provides objective function values to the PSO algorithm.

Particle swarm optimization. In this method, a swarm of particles (population) is, initially, randomly distributed across the design space. The current position of each particle in the swarm (Equation 1) at any point in time is then updated using a velocity vector (Equation 2). Throughout the current work, a unit time step is used ($\Delta t = 1$).

$$x_{i+1}^{p} = x_i^{p} + v_{i+1}^{p}\,\Delta t \tag{1}$$

$$v_{i+1}^{p} = w v_i^{p} + c_1 r_1 \frac{(h_i^{p} - x_i^{p})}{\Delta t} + c_2 r_2 \frac{(h_i^{g} - x_i^{p})}{\Delta t} \tag{2}$$

The above equations are illustrated in Figure 6. Here, x_i^p and v_i^p are the position and velocity of particle p at iteration i; r_1 and r_2 are randomly generated factors ranging from 0 to 1, which differ for each particle and iteration; h_i^p represents the best ever position of particle p where the objective function value is minimum, and h_i^g corresponds to the global best position up to iteration i for the minimal value of the objective function for the whole swarm. w, c_1 and c_2 are optimization parameters limited to the 0–1 range. w is the inertia weight controlling the exploring abilities of the swarm. Large inertia weights allow for global exploration of the design space. c_1 and c_2 are trust parameters indicating, respectively, how much confidence the current particle has in itself and how much in the swarm.

Objective function. Given the multidisciplinary nature of helicopter rotor analyses, the optimization study is proposed to be multi-objective. The following are the objectives selected for this optimization study: total rotor power required, P (performance criterion), blade tip elastic torsion, Φ (structural criterion) and N/rev hub vertical shear, $Fz_{4/rev}$ (vibration criterion). In mathematical terms,

$$f_1(\mathrm{X}) = \mathrm{P};\ f_2(\mathrm{X}) = \Phi;\ f_3(\mathrm{X}) = \mathrm{Fz}_{4/\mathrm{rev}}$$

The rotor power required has been chosen as an objective because the primary goal of the parent project SABRE is to improve the efficiency of the helicopter. The blade tip elastic twist is a critical parameter because it was found to be prohibitively high in the initial morphed designs, because of the change in torsional stiffness. Hence, this parameter was chosen as an objective. The tip elastic twist, being proportional to the root torsional moment, is also indicative of the magnitude of structural loads. The main rotor is the primary contributor of vibratory loads to the fuselage in the form of harmonics of the blade passage frequency. Since the Bo105 rotor, chosen for this work, is 4-bladed, the 4/rev harmonic of its vertical hub load, Fz, is a good measure of its vibratory loads. Thus, three critical aspects of helicopter rotor design, namely, performance, structural loads and vibratory loads, were considered for optimization in this work.

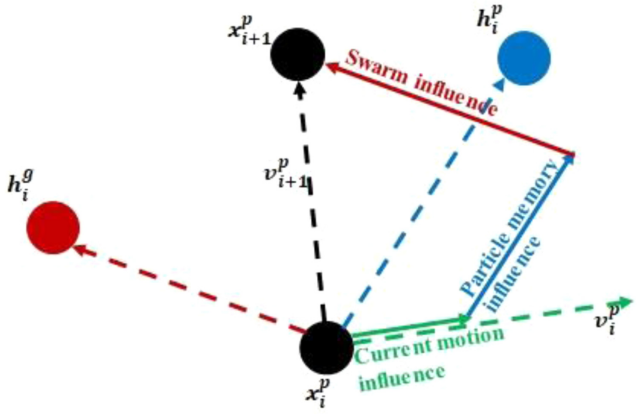


Figure 6. Position and velocity update for a swarm particle.

The multi-objective problem can be converted to a single-objective problem by building a composite objective function using the classical weighted sum method[28] from the individual normalized, weighted objective functions:

$$f = \sum_i \frac{f_i}{f_{ni}} * w_i \qquad (3)$$

where f is the composite objective function; f_{ni} is the normalizing factor; w_i is the weighting factor.

The normalizing factors chosen for the three objective functions are: 350kW (for P), 2.5 deg (for Φ), and 500 N (for $Fz_{4/rev}$).

Design constraints. Constraints are restrictions that must be satisfied to produce an acceptable design. The first requirement set here is that the rotor power required, P, at any velocity for the morphed rotor must be less than the corresponding rotor power (P_{BL}) required for the baseline rotor at that velocity. Φ and $Fz_{4/rev}$ have upper constraints too. Thus,

$$0\ \mathrm{kW} < \mathrm{P} < \mathrm{P_{BL}}$$
$$0\ \mathrm{deg} < \Phi < 5\ \mathrm{deg}$$
$$0\ \mathrm{N} < \mathrm{Fz_{4/rev}} < 1000\ \mathrm{N}$$

Another requirement is that the rotor must be completely trimmed for any flight condition. This constraint is difficult to be translated into a mathematical form. It is implemented as a Boolean relation checking in an S4 output file for trim confirmation.

Design variables. The design variables used are the same as the morphing parameters. In the case of chord-morphing, the design variables and their corresponding limits are:

$$\mathrm{X_c} = \{\mathrm{r_h}, \Delta_c, \alpha_d\}$$

$\mathrm{r_h} \in [0.4 - 0.7]$; $\Delta_c \in [0\% - 100\%]$; $\alpha_d \in [0^o - 15^o]$

The hinge location is limited to a maximum of 0.7 because longer lengths of the rear spar result in higher cross-sectional out-of-plane deformation of the morphed parts of the blade. Hinge locations less than 0.4 do not provide any substantial aerodynamic benefits because of the negligible morphed area. As will be seen in the next section, the dynamic response problem of the rotor is solved in the modal domain. For every change in the rotor structural properties, the modal information has to be recalculated. In order to keep the computational effort to reasonable levels, the design variable domains are discretized as follows:

$\mathrm{r_h} \in [0.4 - 0.7]$ in steps of 0.02

$\Delta_c \in [0\% - 100\%]$ in steps of 12.5%

$\alpha_d \in [0^o - 15^o]$ in steps of 5^o

The following are the design variables for the case of twist morphing –

$$\mathrm{X_t} = \{\mathrm{r_t}, \mathrm{l_t}, \Delta_\theta\}$$

$r_t \in [0.22, 0.39, 0.56, 0.73, 0.9]$; $l_t \in [0.0625, 0.125, 0.1875, 0.25, 0.5, 0.75]$; $\Delta_\theta \in [0.00, 0.22, 0.44, 0.66, 0.88, 1]$

Thus, the first goal of the current optimization study is to find the combination of morphing parameters of a helicopter rotor which minimizes the performance, structural and vibration objective functions subject to some design constraints, for three different chosen mission profiles.

Analysis. It is to be noted that in the case of chord-morphing, the hinge location is a fixed parameter during a mission while the chord-extension and deflection can be changed as desired. These conditions make the morphed rotor optimization a two-level problem. The outer loop (Lo) decides the hinge location, r_h, using a mission-level objective function. Within the outer loop, an inner loop (Li) determines the optimum combination of chord-extension, Δc, and chord-deflection, α_d, for each velocity in a mission using the individual objective function. Thus, the outer and inner loops have their own objective functions and design variables:

Design variables:

$$\mathbf{X_{cLo}} = \{r_h\}; \mathbf{X_{cLi}} = \{\Delta_c, \alpha_d\}$$

Objective function:

Inner loop: $f_1(\mathbf{X_{cLi}}) = P; f_2(\mathbf{X_{cLi}}) = \Phi; f_3(\mathbf{X_{cLi}}) = Fz_{4/rev}$

A composite objective function (f_{Li}) is built using Equation 3.

$$f_{Li} = \sum_i \frac{f_i}{f_{ni}} * w_i \tag{4}$$

This composite function is calculated for each velocity in a mission. Since the three objective functions are dissimilar quantities with different orders of magnitude, they are all non-dimensionalized with appropriate normalizing factors so that they can be summed together. The three objective functions are given equal weightage, $w_i = 0.333$

Outer loop: $f_{Lo} = \sum (f_{Li})_{vi} * w_{vi}$ (5)

The outer loop objective function is calculated as the sum of composite objective functions of all velocities in a mission scaled by weighting factors, w_{vi}, given in Table 2.

Similarly, the case of twist-morphing is also a two-level problem. However here, two parameters, namely, the radial location and the length of the torque-tube are fixed during a mission while the percent twist of the tube can be changed as desired. So r_t and l_t are determined in the outer loop while Δ_θ for each velocity is calculated in the inner-loop:

$$\mathbf{X_{tLo}} = \{r_t, l_t\}; \mathbf{X_{tLi}} = \{\Delta_\theta\}$$

The inner and outer loop objectives for the twist-morphing case are determined in the same manner as for the chord-morphing case.

Following trade-off studies for convergence and duration, 10 particles were chosen as the population for the outer loop and 20 particles for the inner loop. The following values were taken for the optimization parameters (w, c_1, c_2): - (0.4, 0.1, 0.1) for the outer loop and (0.5, 0.2, 0.2) for the inner loop. These values satisfy the PSO parameter selection heuristic in 29.

The Bo105 main rotor blade with the airfoil NACA23012tab was selected as the baseline blade. The parameters for this baseline rotor blade are given in 2. The rotor had a rectangular blade geometry with a radius (R) of 4.92m, blade chord (C) of 0.27m and a linear twist of -8deg. The vehicle was powered by two engines with total power of 626kW. Important structural data distribution for the cross-section of this blade is shown in the Figure 7

Rotor comprehensive analysis. As already mentioned, the comprehensive analysis tool S4, a high resolution, nonlinear, unsteady aerodynamics code with elastic blade structural model, was used for the analysis of the isolated rotor for hover and forward flight conditions. For structural dynamics of the rotor, first, modal analysis was performed using the finite element method (FEM) based on the Houbolt–Brooks formulation[30] which considers flap, lag and torsion degrees for the blade element. For the FEM, a radial resolution of 50 elements was chosen for the rotor blade and for the modal analysis, upto 10/rev natural frequencies were considered with 3-5 flap, 2-3 lag and 1-2 torsion modes. Next, for the dynamic response problem, the blade modes were subjected to generalized aerodynamic forces and generalized coupling forces from other modes like flap-torsion and flap-lag. The response problem was then solved using Runge–Kutta fourth order time-integration method until convergence was achieved. An azimuthal resolution of 1 deg was chosen for the analysis. S4 has an isolated rotor trim module, where the algorithm adjusted the collective pitch and cyclic pitch control inputs and the rotor shaft angle (for forward flight cases) until a trim goal was met.

Since the dynamic response problem was solved in the modal domain, for every change in the structural properties of the blade, a new modal analysis was required. Variation of the morphing parameters / design variables (Table 1) results in variation of structural properties of the blade and these were captured in the form of surrogate models which, essentially, take the form as in Table 3. It is to be noted that the beam formulation remains the same for the morphed blades too since morphing is modelled as only a change in the sectional properties.

The structural properties of the rotor blade at multiple sections were calculated from 3D finite element models which consider the changes in shape of the section. The important changes in the structural properties of the surrogate models of the morphed configurations from those of the baseline blade are given in Refs. 2, 4. In order to reduce the costs of the optimization process, the modal information of all the rotor blades derived from different combinations of the morphing parameters were obtained in advance and used when needed by the code. The discretization of the domain space of the design variables for chord-morphing, as seen in the previous section,

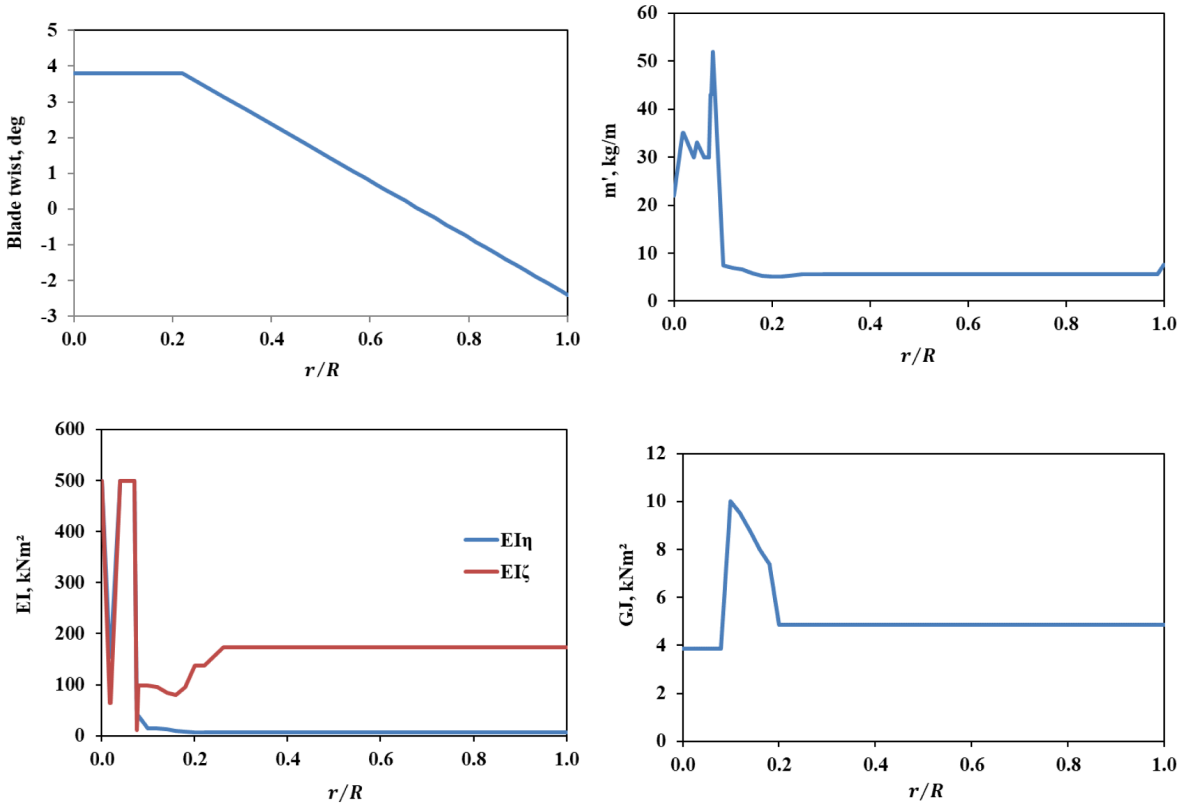


Figure 7. Cross-sectional properties of the baseline BO105 rotor blade.

Table 3. Properties table comprising the surrogate model.

station mo.	r,m	r/R	Θ, deg	m′, kg/m	ef, m	es, m	e0, m	if, m	I_η, m	I_ζ, m	EI_η, Nm²	EI_ζ, Nm²	EB_1, Nm⁴	EB_2, Nm³	GJ, Nm²

resulted in 16 x 9 x 4 = 576 surrogate models; while for twist-morphing, discretization resulted in 5 x 6 x 6 = 180 surrogate models.

Since chord-morphing resulted in a change of shape of the baseline NACA23012tab airfoil, each such case had to be treated as a new airfoil. As reported in 2, extensive CFD calculations were made for the two-dimensional aerodynamic coefficients of the modified airfoils in viscous mode over the range of Mach numbers and angles of attack expected to be experienced by the morphed sections of the rotor. Based on this fresh CFD data, unsteady aerodynamic formulation was synthesized for the aerodynamic coefficients as a function of the morphing parameters. The DLR unstructured Navier-Stokes solver TAU was used for all CFD computations[31,32]. The modified airfoil profile data was obtained from CAD models of the rotor blade and input to TAU. The test matrix for the computations was developed as below.

Test Matrix. Figure 8 shows the velocities experienced by different sections of the rotating rotor on the advancing and retreating sides in hover and in forward flight. The red triangle in the figure represents the chord-extension and spans from 0.22R – 0.6R. As can be seen in Figure 8b, the innermost parts of the rotor with chord-extension might experience reverse flow in the retreating side during forward flight.

As an illustration, for a 100% maximum chord-extension rotor at 70m/s, Table 4 shows the Mach numbers experienced by different spanwise sections on the advancing and retreating sides.

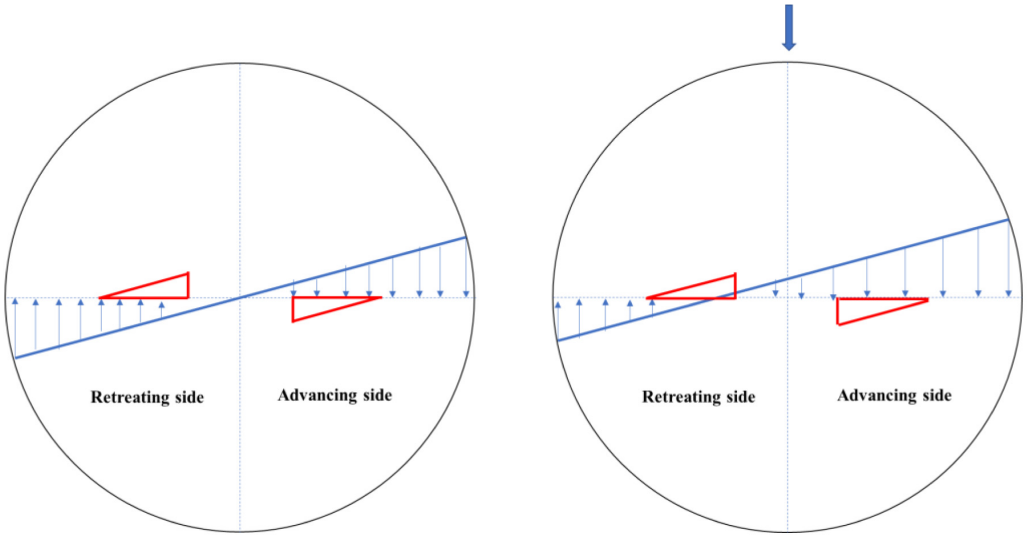


Figure 8. Sectional in-plane velocity distribution for the rotor blade.

Table 4. Maximum and minimum Mach numbers.

Cext	r/R	Mach no at max trim velocity	
		Advancing side	Retreating side
100%	0.22	0.36	-0.07
75%	0.32	0.42	0.00
50%	0.41	0.48	0.06
25%	0.51	0.55	0.12
0%	0.60	0.61	0.18

Table 5. Test Matrix.

Mach no ↓	Chord-extension →					
		0%	25%	50%	75%	100%
	-0.2	x	x	x	x	x
	0.2	x	x	x	x	x
	0.4	x	x	x	x	x
	0.5	x	x	x		
	0.6	x	x			

Based on the illustration above, the following test matrix (Table 5) was setup for optimal CFD calculations. Five different chord-extension sections were considered. Each chord-extension case, apart from the 0%, included chord-deflections of 0 deg, 7.5 deg and 15 deg. It is to be noted that the 0% chord-extension rotor is aerodynamically the same as the baseline rotor. Also, negative Mach number indicates flow from trailing edge towards leading edge. The airfoil was given a slow sinusoidal pitching input for the analysis.

The unsteady aerodynamic formulation in S4 is based on the Leiss model[33,34] where the aerodynamic equations are built from experimental data by superposition of three physical force sources resulting from fully separated flow as per Newton's law, the separated circulatory flow, and the attached circulatory flow. Wagner and Kuessner functions were used to account for circulation lag effects in unsteady motion while dynamic stall is accounted for through a shift of the point of the static angle of attack assuming harmonic oscillation of the airfoil. This new formulation was then incorporated into S4. It is to be noted that such an exercise of deriving a new aerodynamic formulation is not required for twist-morphing because it does not result in a change of the airfoil shape.

S4 has been thoroughly validated as can be seen from literature. Data from wind tunnel experiments in the HART II test campaign, which utilized a hingeless Bo105 scaled model rotor, were used to corroborate the blade motion and sectional air loads of S4[26,27]. The unsteady aerodynamic model for the baseline NACA23012tab airfoil in S4 was derived from data obtained from wind-tunnel tests. The new unsteady aerodynamic model in S4 which was synthesized from data obtained by CFD for the SABRE project was validated for performance and

loads[35] using data from test campaigns carried out at the NASA Ames Research Center 40-by-80-foot wind tunnel, utilizing the full-scale Bo 105 rotor[36]. The Mangler-Squire inflow model was used for the comprehensive analysis as noted in Ref. 2. The overall trends of the results from S4 have been found to be in good agreement with the test data.

Results

For the three missions, two scenarios were considered here – the first one was a simplified single-objective scenario where only the rotor power consumption was taken as the objective function for the inner loop. The second scenario had the composite objective function (Equation 1) calculated from multiple objectives for the inner loop with equal weightages given for all the objectives.

For comparison purposes, the objective function values for the baseline rotor for a range of velocities from hover to fast forward flight are shown in Table 6. The rotor power, P, followed the familiar bucket curve profile with minimum power required at around 30m/s velocity. The blade tip elastic twist, Φ, gradually increased from hover to high speed. The 4/rev harmonic of vertical hub load, $Fz_{4/rev}$, was negligible at hover and was maximum at low speed transition flight at around 30m/s.

Linearly variable chord morphing

Scenario 1. Figures 9 show variation of the outer loop objective function (P) with hinge location for the three different missions. To recall, the outer loop objective function calculated the overall mission objective by summing the weighted global objectives at each velocity in the mission.

The three missions showed similar trends. As the hinge location goes outboard, the required rotor power (P) was seen to reduce. This can be explained by the increase in the surface area of the blade which reduces the overall required angle of attack by the rotor blade[2]. The optimal hinge location was seen to be at around 0.64 for all the three missions. Among the three missions, mission 1 had the least power requirement. This is because of the longer low speed flight duration (bucket region in the power curve). Even though the limit of the hinge location was till 0.7, locations near this outboard region were not seen here because one or more of the design constraint conditions were not met for these values.

Scenario 2. Figure 10 also show the variation of the outer loop objective function with hinge location for the three

Table 6. Baseline rotor.

Velocity, m/s	μ	P, kW	Φ, deg	$Fz_{4/rev}$, N
0	0.0	370	0.46	17
10	0.05	308	0.42	99
20	0.09	238	0.43	594
30	0.14	230	0.53	734
40	0.18	255	0.68	629
50	0.23	310	0.88	473
60	0.27	403	1.15	371

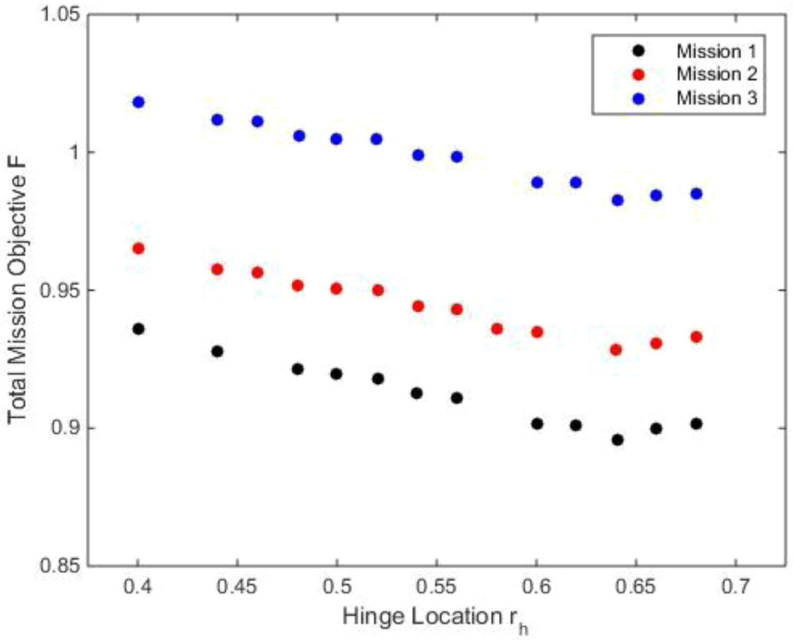


Figure 9. Variation of total mission objective with hinge location in Scenario 1.

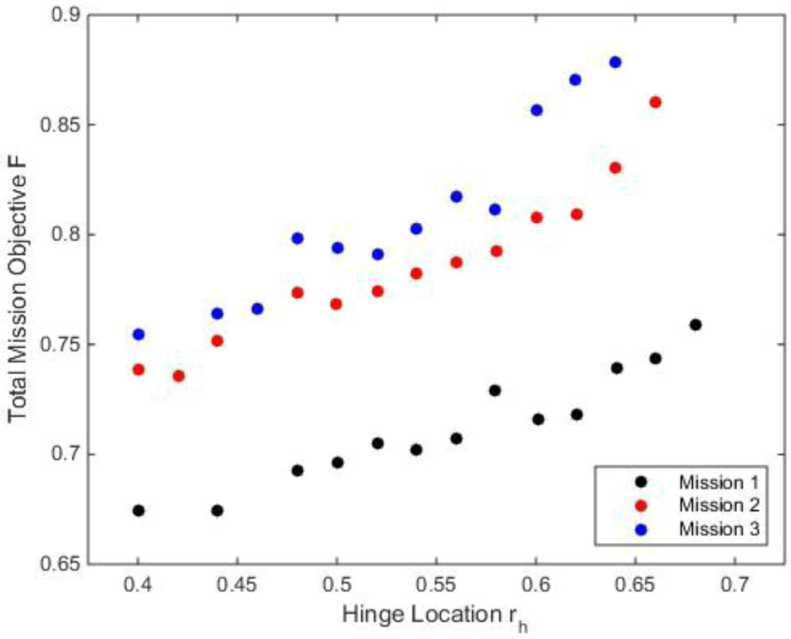


Figure 10. Variation of total mission objective with hinge location in Scenario 2.

different missions. The objective function used here included the tip elastic twist (Φ) and the hub vertical shear 4/rev harmonic ($Fz_{4/rev}$) apart from the required rotor power (P). All three objectives were given equal weightages.

Even though there were slight deviations, the general trend for all three missions was that the optimum was seen to be moving towards the inboard hinge locations. The optimum hinge locations for all three cases were in the region between 0.4 and 0.45. Mission 1, which had a high percentage of hover and low speed flight, had lower mission objectives because of the lower tip twist and vibratory harmonics at these speeds. The observed deviations could be because of the trim calculations in batch mode which had uniform criteria for all velocities. As a result, some of the cases may not be fully trimmed resulting in slight deviations of the values of the objective functions.

Other observations. Mission 2 was selected for further exploration since it had low and high speeds of similar duration. Table 7a–Table 7b show the variation of the optimal morphing parameters for each velocity leg in mission 2 for scenario 1 and scenario 2, respectively.

For scenario 1, a hinge location of 0.64 was found to be the optimal value for the mission. For this hinge location, Table 7a suggests full chord extension for hover and lower velocities for optimum performance and almost nil chord extension for higher velocities. Chord deflections were zero for all velocities. This is because chord deflections resulted in at least one of the design constraints not being satisfied. Comparing with Table 6, it can be seen that the blade tip elastic twist values were much higher than the baseline blade values for this scenario. High blade elastic torsion would require higher pilot collective input angles to offset them and so can be a limiting factor. The vibratory loads were seen to be lower than those for the baseline case. For this mission, compared to the baseline case, the highest power reduction of 6.9% was seen at hover. The overall power required curve for a helicopter in forward flight is bucket shaped which means that it initially reduces as forward speed increases and increases again at higher speeds. The decrease in the power saving from hover to μ=0.14 is due to the lower baseline value at μ=0.14. For higher forward speeds, since chord extension is hardly used, the power reduction was more from changes in the blade structural properties. The overall power reduction for the entire mission was calculated considering the weightages of the individual speeds and was found to be 4.2% for this case.

For scenario 2 (Table 7b), the optimal hinge location for the mission was at 0.42. The tip elastic twist values were closer to those of the baseline blade values which was a highly positive outcome. Similarly, the vibratory loads were also in the same range as the baseline blade. However, the power required had hardly changed from the baseline values, the reason being an inadequate increase in the morphed area of the blade. This scenario shows that high performance along with reduction in tip elastic twist cannot be achieved merely through hinge-location variance.

To summarize the above findings, for the chord-morphing concept, larger chord-extensions are recommended for hover and low speed flights from a performance perspective. For high-speed flights, lower chord-extensions are recommended. Chord-deflections are not recommended for any flight velocity.

Table 7a. Mission 2, Scenario 1, morphing parameters.

r_h	μ	Δ_c, %	α_d, deg	P, kW	Φ, deg	$Fz_{4/rev}$, N	P, % savings
0.64	0	100	0	345	4.7	20	6.9
	0.14	100	0	219	4.5	556	4.7
	0.18	6	0	249	1.5	694	2.5
	0.27	0	0	387	2.0	292	3.8

Table 7b. Mission 2, Scenario 2, morphing parameters.

r_h	μ	Δ_c, %	α_d, deg	P, kW	Φ, deg	$Fz_{4/rev}$, N	P, % savings
0.42	0	6	0	370	0.7	18	0.0
	0.14	20	0	230	0.8	643	0.0
	0.18	0	0	255	0.8	568	0.0
	0.27	0	0	402	1.4	338	0.1

A hinge location close to 0.64 can give decent power savings if the blade tip elastic twist can be reduced through careful design by considering factors such as torsional stiffness of the blade in the inboard regions, offset of the shear center from the pitching axis, and geometric twist of the blade.

Twist morphing

Scenario 1. For the twist case, there are two outer loop design parameters which need to be fixed for a mission – the radial location of the twist tube (r_t) and the length of the twist tube (l_t). Figures 11a–c show the variation of the outer loop mission objective function with respect to the radial location of the twist tube, r_t ($i1$). Each radial location had multiple values of the total mission objective, each corresponding to a different value of the length of the twist tube, l_t ($i2$). Only the minimal values for the radial locations were of interest here (the ones marked in red), the other data points were shown only for completeness and may be glossed over. For the three missions, the optimal mission objective occurred at radial locations of the twist tube at 0.56. As the high-speed velocity duration increased in a mission, the mission objective function was also seen to rise.

Figures 12a–c show the variation of the mission objective with respect to the twist tube length for the three missions. The multiple values for each tube length, which have been given only for completeness, correspond to a different value of tube radial location. Only the minimal values were of interest here (the ones marked in red). Tube lengths of 0.5 and 0.75 were seen to give the optimum results.

Scenario 2. Figure 13a–c and Figure 14a–c show the same information as above for scenario 2, where the effect of Φ and $Fz_{4/rev}$ were included with equal weightage as the rotor power. Only the points marked in red may be considered here. Observing the two sets of plots, it can be concluded that for all the missions, the requirement of optimal elastic twist and vibration shortened the torque-tube lengths to 0.06235 or 0.125 and placed the tube locations more inboard.

Table 8a, Table 8b shows the variation of optimal morphing parameters for mission 2 for twist morphing. Table 8a gives the values for scenario 1. It was concluded earlier from Figure 11 and Figure 12 that the optimal radial location of the twist tube was 0.56 and the optimal length of the tube was 0.75. For these fixed values, the delta twist of the tube was seen to decrease as the forward velocity increased. For hover, the full delta was required while for high speeds 22% twist was sufficient. The percentage reduction in rotor power was lower than that for the chord morphing case. For mission 2, at hover, there was a reduction of 11.6% in rotor power compared to the baseline rotor. The overall power reduction for the entire mission was about 3.5%. Vibratory loads were comparable to those of the baseline values. Tip elastic twist, while it was higher than the baseline values, was lower than those for the chord morphing case.

Table 8b gives the optimal morphing parameter values when Φ and $Fz_{4/rev}$ were also considered in the objective function. A radial location of 0.22 was recommended together with a tube length of 0.0625 for this scenario. The delta twist was higher for forward velocities. Even though the tip elastic twist was brought down close to the baseline values, this scenario was of no significant benefit since the power saving compared to the baseline case was negligible.

To summarize the above results, outboard radial locations of 0.56 and 0.73 for the twist tube gave decent reduction in the

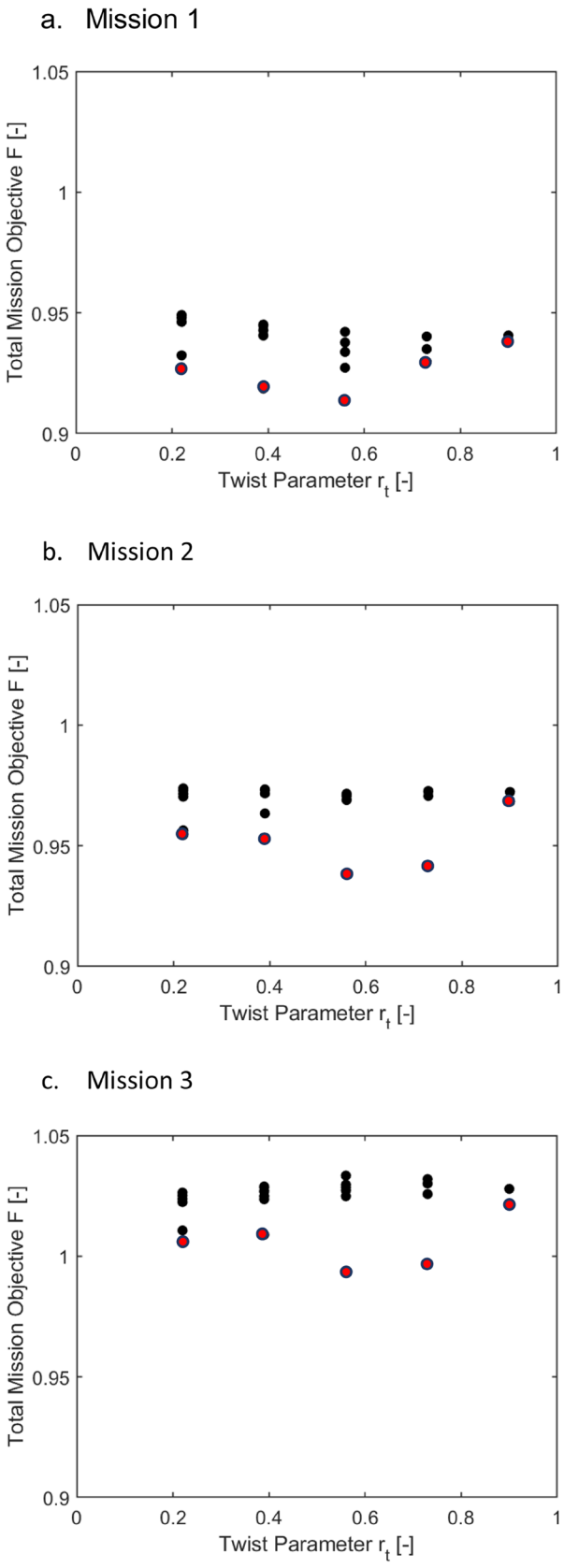


Figure 11. Variation of total mission objective with i1 (r_t) in Scenario 1.

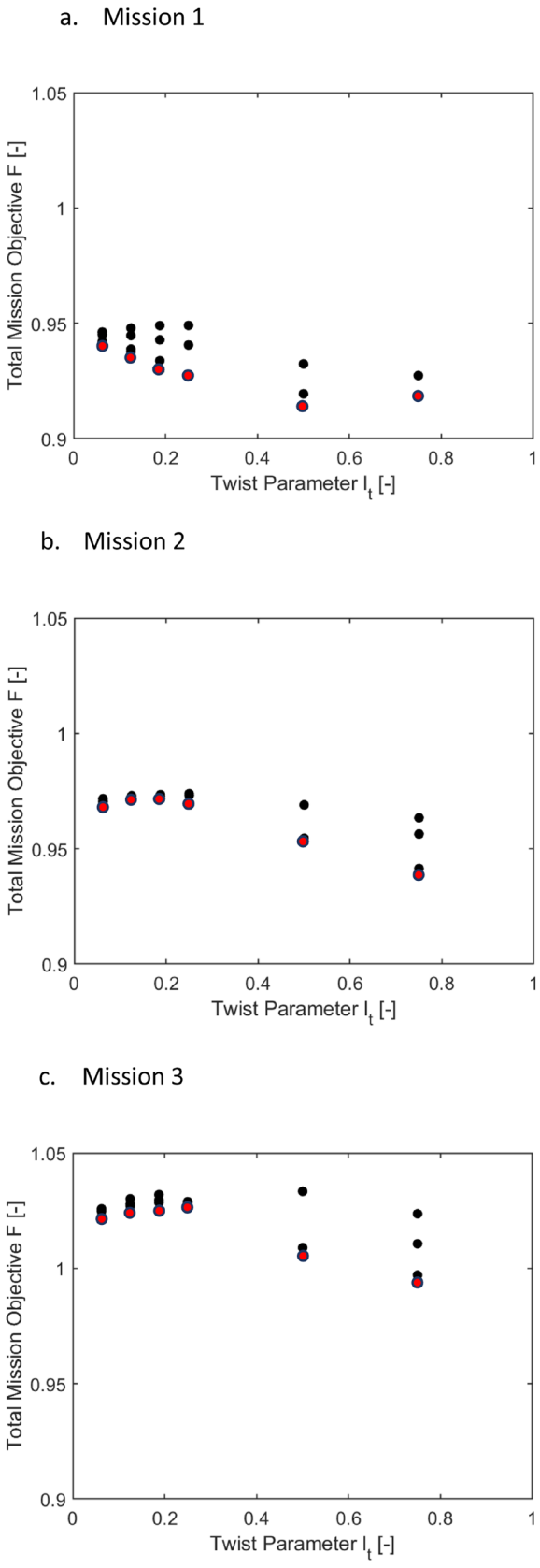


Figure 12. Variation of total mission objective with i2 (l_t) in Scenario 1.

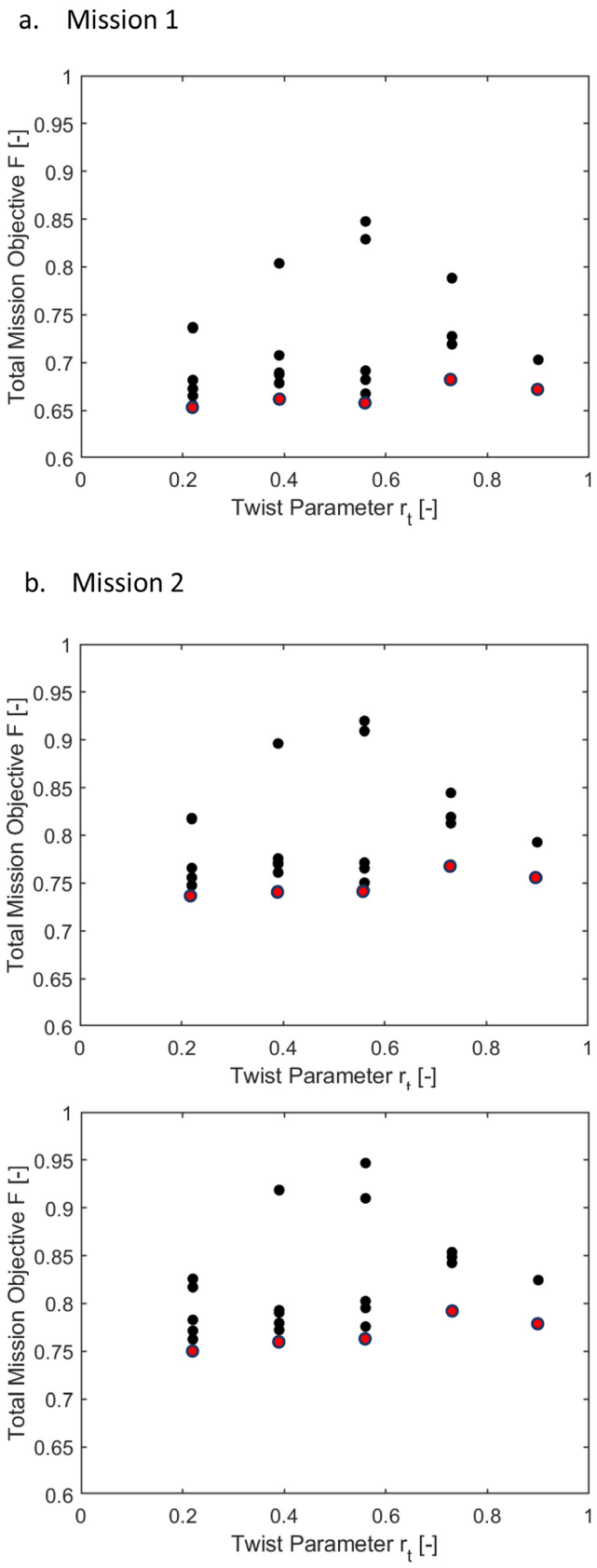


Figure 13. **Variation of total mission objective with i1(r_t) in Scenario 2.**

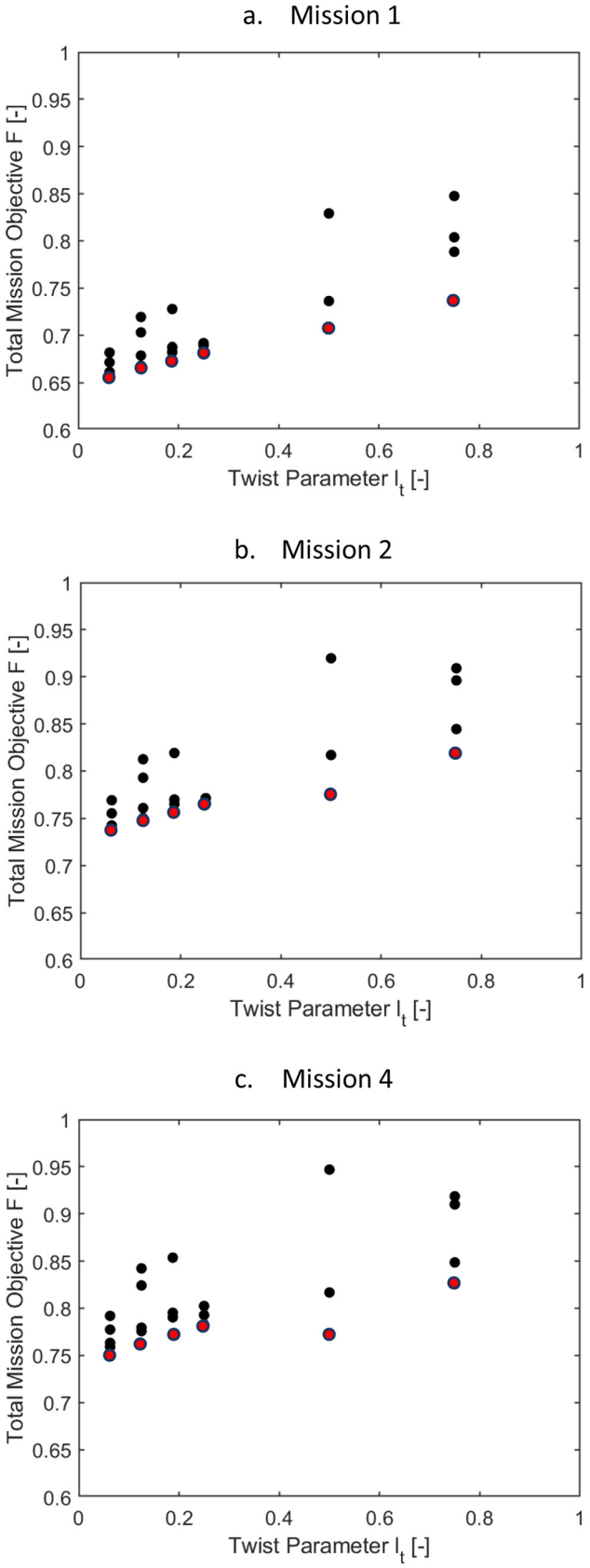


Figure 14. **Variation of total mission objective with i2 (l_t) in Scenario 2.**

rotor power albeit with slightly high elastic twist of the blade. Shorter lengths of the twist tube could be used to reduce the tip elastic twist.

Combined chord and twist morphing

Based on the trends observed in the previous sections, it can be seen that the optimal configurations of the two morphing concepts could be easily integrated into a single blade with minimal overlapping as shown in Figure 15. From a structural design point of view, it was decided to limit the chord-morphing hinge location to 0.6 in order to reduce the out-of-plane deflection of the morphed airfoil sections. For the twist tube, it was decided to have a length of 0.125 at location 0.73 due to structural constraints. The non-variable morphing parameters for the mission were thus set. For the combined configuration, the inner and outer loop design vectors are a concatenation of the vectors of the individual case. The rest of the problem formulation and solution is the same as in the individual morphing cases.

$$\mathbf{X_{ctLo}} = \{r_h, r_t, l_t\};\ \mathbf{X_{ctLi}} = \{\Delta_c, \alpha_d, \Delta_\theta\}$$

Figure 16 shows a comparison of the power required, tip elastic twist and the vertical hub vibration for the combined morphing blade (subscript 'ct') with the baseline blade and the stand-alone chord morphing blade (subscript 'c'). The rotor with the combined morphing concept compared favorably with the baseline rotor. The power required (green) was less than that for the baseline blade (blue) throughout the mission. The net effective power savings for the complete mission with respect to the baseline blade was 6.8% which was an improvement over the stand-alone chord morphing concept (4.2%). The power saving was higher at 13% for hover and low speed flight of μ = 0.14. The tip elastic torsion for the combined morphing blade, though higher than that for the baseline blade, was also lower compared to the stand-alone chord morphing case in scenario 1. The hub vibrational loads compared very favorably with the baseline case.

Table 8a. Mission 2, Scenario 1, morphing parameters.

μ	Δ_θ, deg	P, kW	Φ, deg	$Fz_{4/rev}$, N	P, % savings
0	1	327	2.4	39	11.6
0.14	0.44	228	1.7	877	0.9
0.18	0.22	254	1.7	632	0.4
0.27	0.22	392	2.4	408	2.7

Table 8b. Mission 2, Scenario 2, morphing parameters.

μ	Δ_θ, deg	P, kW	Φ, deg	$Fz_{4/rev}$, N	P, % savings
0	0.22	368	0.5	18	0.5
0.14	0.22	230	0.6	740	0.0
0.18	0.22	255	0.7	633	0.0
0.27	0.22	403	1.2	381	0.0

The reduction in required power, shown in Figure 16, can be understood by comparing the angle of attack distribution of the three rotors in hover. Figure 17 shows the radial distribution of the angle of attack of the baseline rotor, the chord-morphing rotor and the combined-morphing rotor at the 90° azimuth. Note that for the stand-alone chord-morphing rotor, chord extension was 100% while for the combined-morphing rotor, chord extension was 50%. For the chord-morphing case, the sections from r = 0.35R till r = 0.95R had less angles of attack than those for the baseline case. On average, the reduction was about 0.5°. This reduced the profile drag of a rather large part of the rotor blade and hence, reduced the overall required power. In the combined-morphing rotor, the variation of the angle of attack across the blade was redistributed with a sharp reduction in the final 25% of the blade after the torque-tube. On average, the reduction from the baseline blade was about 1.2° in this region. To compensate for the reduced lift in this region, the angles of attack in the inboard 50% of the blade (from r = 0.28R to r = 0.70R) show an average increase of 1.2°, thus increasing the lift in this region. The profile drag of a rotor blade had its highest contribution from the outboard region where the dynamic pressure was the highest. For the combined-morphing blade, profile drag in the outboard region was drastically reduced because of the low angles of attack, thus reducing the overall power required.

With regards to the Fz4/rev component, taking a closer look at the μ=0.27 case might be warranted because of the drastic fall in the values of the combined morphing case from those of the baseline case. A plot of all the force components (Figure 18) reveals that even though the z-component has reduced, it is

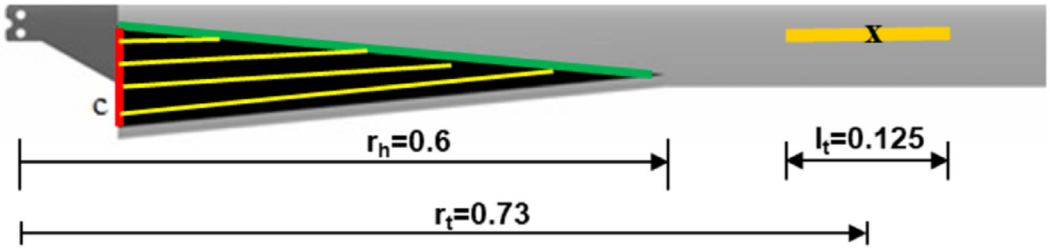


Figure 15. Combined morphing concept.

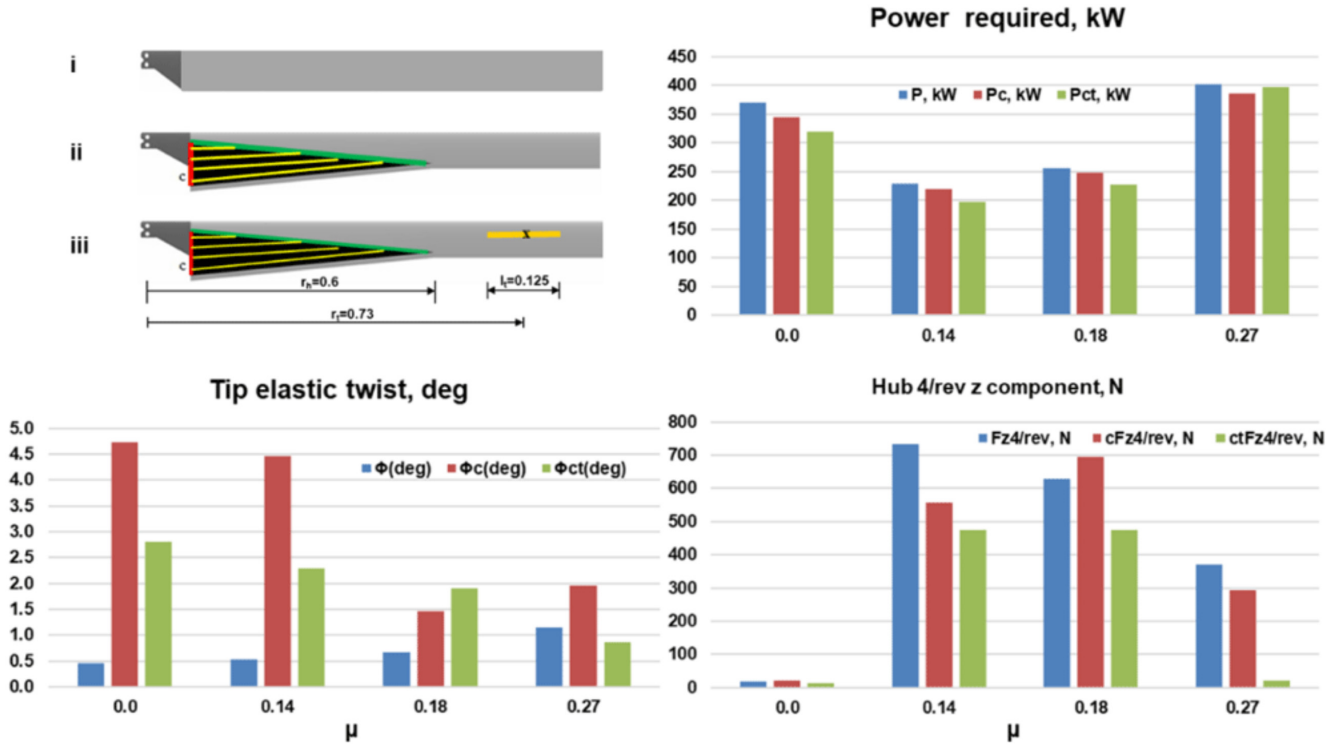


Figure 16. Comparison of rotor analysis results for the baseline, stand-alone chord morphing and the combined morphing blades.

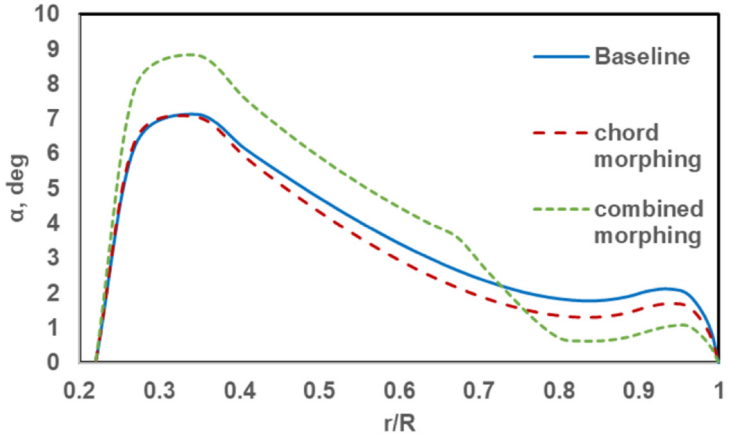


Figure 17. Radial distribution of angle of attack in hover.

accompanied by a large rise in the x-component. The root mean square of the three components gives a value of 507N for the baseline case and 560N for the combined morphing case.

It was observed in the Campbell diagrams of the lower chord-extension blades that there was a strong flap-torsion coupling at rotor design speed. This resulted in lower chord-extension rotors not trimming at high speeds. With further design changes to prevent the flap-torsion coupling at rotor design speeds, it should be possible to have higher power savings with the combined morphing concept.

Conclusions

Linearly variable chord morphing and torque-tube twist morphing for helicopter rotor blades were studied for their mission-based optimal geometric parameters. For this, an

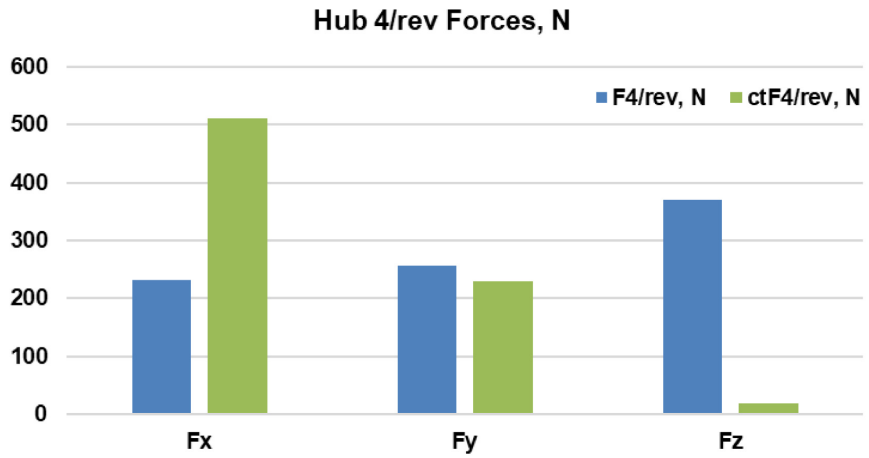


Figure 18. Components of the hub 4/rev forces for the baseline and combined morphing cases.

evolutionary algorithm, PSO, was combined with a high- resolution helicopter rotor comprehensive analysis code, S4. A fully elastic rotor blade was modelled in an unsteady aerodynamic environment. It was found that the two concepts could have non-overlapping optimal conditions. By combining both concepts into a single rotor blade, better performance than the baseline blade was achieved, while the penalty in elastic torsion and hub vibrational load were within reasonable limits. The combined concept also gives better performance than the individual stand-alone concepts. A couple of factors which limit the performance of the combined concept blade are to be noted: one is the flap-torsion coupling at the design rotor speed for the lower chord-extension cases. The other factor is the low torsional stiffness of the chord-morphing region of the blade, which resulted in high elastic twist in the blade. Improving these two design aspects can result in smoother trends in the optimization results, and can lead to further improvements in the rotor efficiency. In addition, more stringent criteria such as including all the components of hub vibratory loads in the objective function would lead to a better design.

Abbreviations

BL	Baseline
Lo, Li	Outer loop and inner loop abbreviations
f_1, f_2, $f_3(X)$	Individual objective functions
f_i, f_{ni}	The indexed objective function and corresponding normalizing factor
f	The composite objective function
w_i	Weighting factor for objective function
h_i	Best position at iteration i of optimization loop
xi, vi	Position and velocity at iteration i of optimization loop
p, g	Superscripts indicating particle-level and global-level values
w, c_1, c_2	Optimization parameters used in the PSO velocity equation
r_1, r_2	Random numbers between 0-1
w_{vi}	Weightage of a mission leg
C	Chord length of baseline blade, m
$Fz_{4/rev}$	4/rev harmonic of vertical hub load, Fz
P	Main rotor required power, kW
Φ	Blade tip elastic twist, deg
α	Angle of attack, deg
μ	Advance ratio
r	Rotor blade radius variable, m
R	Radius of rotor, m
i1, i2, i3	Morphing parameters index
r_h	Non-dimensional radial location of hinge wrt R
α_d	Chord deflection, deg
Δ_c	Maximum chord extension as a percentage of baseline chord, C
l_t	Torque-tube length, non-dimensional wrt R
r_t	Radial location of torque-tube center
Δ_θ	Percent twist of torque-tube
Δ_{max}	Maximum twist of torque-tube
X_c, X_t	Design variable vectors for chord-morphing and twist-morphing
m’	Mass per unit span of the blade, kg/m
ef	Offset of the tension axis to the elastic axis, m
es	Offset of the center of gravity axis to the elastic axis, m

e0	Offset of the pitch axis to the elastic axis at the blade root, m
if	Polar radius of gyration of the cross-section area with respect to the elastic axis, m
I_η	Flapping polar radius of gyration of the cross-section mass distribution about the local chord line, m
I_ζ	Lagging polar radius of gyration of the cross-section mass distribution about axis normal to the chord line, m
EI_1	Flap bending stiffness about the local chord line, Nm^2
EI_2	Lag bending stiffness about the axis normal to the chord line, Nm^2
EB_1	Radial stiffness term associated with twist, Nm^4
EB_2	Radial stiffness term associated with bending, Nm^3
GJ	Torsional stiffness about the axis normal to the plane of the local cross-section, Nm^2

Data availability

Underlying data

The program and part of the data (pertaining to structural properties of the chord-morphed sections) used in this work are owned by the lead author's employer, the German Aerospace Center (DLR), and are restricted by the organization to internal use only. Other data (structural properties of the baseline blade and those of the twist-morphed sections) are held under restriction by third parties and are not available for publication. All data underlying the results and necessary for review are available as part of the article or in relevant references.

Acknowledgements

For some of the calculations, data received from CIRA, Italy was used and for this the authors are grateful.

References

1. Rauleder J, van der Wall BG, Abdelmoula A, *et al.*: **Aerodynamic Performance of Morphing Blades and Rotor Systems.** *AHS 74th Annual forum & Technology Display.* Phoenix, AZ, USA, May 2018.
Reference Source
2. Majeti RK, van der Wall BG, Balzarek CG: **Linearly Variable Chord-Extension Morphing for Helicopter Rotor Blades. 12**: 55–67.
Publisher Full Text
3. Ameduri S, Concilio A: **An SMA Torsion Actuator for Static Blade Twist**. *Proceedings of the 29th International Conference on Adaptive Structures and Technologies.* Seoul, South Korea, Oct. 2018.
4. Ameduri, S, Concilio A, Majeti RK: **An FE Based Surrogate Model for Predicting the Impact of a SMA Twist System on the Helicopter Performance**. *Proceedings of the ASME 2019 Conference on Smart Materials, Adaptive Structures, and Intelligent Systems.* Louisville, KY, USA, Sept. 2019.
Publisher Full Text
5. Komp D, Kumar S, Hajek M, *et al.*: **Effect of active camber morphing on rotor performance and control loads.** *Aerosp Sci Technol.* 2021; **108**: 106311.
Publisher Full Text
6. Balzarek C, Kalow S, Riemenschneider J, *et al.*: **Manufacturing and Testing of a Variable Chord Extension for Helicopter Rotor Blades**. In *Actuators.* MDPI, 2022; **11**(2): 53.
Publisher Full Text
7. Concilio A, Dimino I, Lecce L, *et al.*: **Morphing wing technologies: Large commercial aircraft and civil helicopters**. Butterworth-Heinemann. 2017.
Reference Source
8. Walsh JL, Bingham GJ, Riley MF: **Optimization methods applied to the aerodynamic design of helicopter rotor blades.** *J Am Helicopter Soc.* 1987; **32**(4): 39–44.
Publisher Full Text
9. Volovoi V, Li L, Ku J, *et al.*: **Multi-level structural optimization of composite rotor blades**. In *46th AIAA/ASME/ASCE/AHS/ASC Structures, Structural Dynamics and Materials Conference.* 2005; 2282.
Publisher Full Text
10. Callahan CB, Straub FK: **Design Optimization of Rotor Blades for Improved Performance and Vibration.** *Journal of the American Helicopter Society.* 1993; **38**(4): 62–70(9).
Publisher Full Text
11. Walsh JL, Young KC, Pritchard JI, *et al.*: **Multilevel decomposition approach to integrated aerodynamic/dynamic/structural optimization of helicopter rotor blades**. *Proceedings of the AHS Specialists' Conference on Aeromechanics.* San Francisco, CA USA, 1994.
Reference Source
12. Collins K, Bain J, Sankar L, *et al.*: **Pareto Frontier Method for Multi-Disciplinary Optimization of Helicopter Rotors**. *Proceedings of the AHS Specialists' Conference on Aeromechanics.* San Francisco, CA, USA, Jan. 2008.
Reference Source
13. Viswamurthy SA, Ganguli R: **Optimal placement of piezoelectric actuated trailing-edge flaps for helicopter vibration control.** *J Aircr.* 2009; **46**(1): 244–253.
Publisher Full Text
14. Glaz B, Goel T, Liu L, *et al.*: **Multiple-surrogate approach to helicopter rotor blade vibration reduction.** *AIAA Journal.* 2009; **47**(1): 271–282.
Publisher Full Text
15. Kumar D, Cesnik CE: **New strategy for designing composite rotor blades with active flaps.** *Journal of Intelligent Material Systems and Structures.* 2016; **27**(9): 1176–1188.
Publisher Full Text
16. Kumar D, Cesnik, CE: **New optimization strategy for design of active twist rotor.** *AIAA Journal.* 2015; **53**(2): 436–448.
Publisher Full Text
17. Jasa JP, Hwang JT, Martins JR: **Design and trajectory optimization of a morphing wing aircraft**. In *2018 AIAA/ASCE/AHS/ASC Structures, Structural Dynamics, and Materials Conference.*2018; 1382.
Publisher Full Text
18. Rao SS: **Engineering Optimization: Theory and Practice, Fourth Edition.** John Wiley and Sons, Inc, New Jersey, NJ, USA, 2009.
Publisher Full Text
19. Eberhart RC, Shi Y: **Particle swarm optimization: developments, applications and resources**. *Proceedings of the Congress on Evolutionary Computation (IEEE Cat. No. 01TH8546)*. IEEE, Seoul, South Korea, May 2001; 81–86.
Publisher Full Text
20. Guglieri G: **Using of Particle Swarm for Performance Optimization of Helicopter Rotor Blades.** *Applied Mathematics.* 2012; **03**(10): 1403–1408.
Publisher Full Text
21. Ramanujam R, Abhishek A: **Performance optimization of variable-speed and variable-geometry rotor concept.** *Journal of Aircraft.* 2017; **54**: 476–489.
Publisher Full Text
22. Benz S, Majeti RK: **Optimization of a Rotor with Morphing Blades using Particle Swarm Algorithm**. *Proceedings of the German Aerospace Congress.* DLRK, Darmstadt, Germany, Sept. 2019.
23. Gessow A, Myers GC: **Aerodynamics of the Helicopter.** Frederick Ungar Publishing Co, New York, NY USA, Third edition, 1967.
Reference Source

24. Crossley WA, Laananen DH: **Conceptual design of helicopters via genetic algorithm.** *Journal of Aircraft.* 1996; **33**(6): 1062–1070.
Publisher Full Text

25. Karamolegkos K, Goulos I, Pachidis V, *et al.*: **Helicopter mission analysis using a multidisciplinary simulation framework.** *Proceedings of the ASME Turbo Expo,* Vol. 1A, Düsseldorf, Germany, June 2014.
Publisher Full Text

26. van der Wall BG, Yin J: **DLR's S4 Rotor Code Validation with HART II Data: The Baseline Case.** International Forum on Rotorcraft Multidisciplinary Technology, Seoul, South Korea, Oct. 2007.

27. van der Wall BG, Lim JW, Smith M, *et al.*: **The HART II International Workshop: An Assessment of the State-of-the-Art in Comprehensive Code Prediction.** *CEAS Aeronautical Journal.*2013; **4**(3): 223–252.
Publisher Full Text

28. Deb K: **Multi-objective optimization using evolutionary algorithms.** Wiley, Chichester, UK, 2001.
Reference Source

29. Perez RE, Behdinan K: **Particle swarm approach for structural design optimization.** *Journal of Computers and Structures.* 2007; **85**(19– 20): 1579–1588.
Publisher Full Text

30. Houbolt JC, Brooks GW: **Differential equations of motion for combined flapwise bending, chordwise bending, and torsion of twisted nonuniform rotor blades.** In: NACA TN 1957; **3905**.
Reference Source

31. Gerhold T, Friedrich O, Evans J, *et al.*: **Calculation of Complex Three-Dimensional Configurations Employing the DLR-TAU-Code**. *AIAA-paper 97-0167, 35th AIAA Aerospace Sciences Meeting & Exhibit.* Reno, NV, Jan. 6–9, 1997.
Publisher Full Text

32. Schwamborn D, Gardner AD, von Geyr H, *et al.*: **Development of the TAU-Code for aerospace applications**. 50th NAL International Conference on Aerospace Science and Technology, Bangalore, India, 2008.
Reference Source

33. Leiss U: **A consistent mathematical model to simulate steady and unsteady rotor-blade aerodynamics.** In: *10th European Rotorcraft Forum,*. The Hague, Netherlands, 1984.

34. van der Wall BG: **An Analytical model of unsteady profile aerodynamics and its application to a rotor simulation program.** In: *15th European Rotorcraft Forum*, Amsterdam, Netherlands, 1989.

35. Benz S: **Validation of S4 using Simple Inflow Models.** DLR Internal Report. DLR-IB-FT-BS-2019-192, 2019.
Reference Source

36. Peterson RL: **Full-scale Hingeless Rotor Performance and Loads.** Technical Report 110356 NASA TM, 1995.
Reference Source

Open Peer Review

Current Peer Review Status: ✔ ✔

Version 2

Reviewer Report 14 June 2022

https://doi.org/10.21956/openreseurope.16049.r29481

© **2022 Shen W.** This is an open access peer review report distributed under the terms of the Creative Commons Attribution License, which permits unrestricted use, distribution, and reproduction in any medium, provided the original work is properly cited.

✔ **Wen Zhong Shen**
College of Electrical, Energy and Power Engineering, Yangzhou University, Yangzhou, China

The authors answered all my questions with satisfaction and I have no further comments.

Competing Interests: No competing interests were disclosed.

I confirm that I have read this submission and believe that I have an appropriate level of expertise to confirm that it is of an acceptable scientific standard.

Reviewer Report 14 June 2022

https://doi.org/10.21956/openreseurope.16049.r29482

© **2022 Hajek M.** This is an open access peer review report distributed under the terms of the Creative Commons Attribution License, which permits unrestricted use, distribution, and reproduction in any medium, provided the original work is properly cited.

✔ **Manfred Hajek**
Institute of Helicopter Technology, Technical University of Munich, Munich, Germany

I have read the new version and checked the authors' response to my comments. Sufficient improvement has been made so that I can agree to indexing without further request for modification.

Competing Interests: No competing interests were disclosed.

I confirm that I have read this submission and believe that I have an appropriate level of expertise to confirm that it is of an acceptable scientific standard.

Version 1

Reviewer Report 27 October 2021

https://doi.org/10.21956/openreseurope.15151.r27792

© **2021 Hajek M.** This is an open access peer review report distributed under the terms of the Creative Commons Attribution License, which permits unrestricted use, distribution, and reproduction in any medium, provided the original work is properly cited.



Manfred Hajek
Institute of Helicopter Technology, Technical University of Munich, Munich, Germany

General remarks:
The paper lacks a discussion of the state of the art in order to clearly identify where the authors' contribution is complementary to the publications in the literature list. This is an essential element of good practice in scientific writing.

Detailed comments per page:
Page 1:
- First line: add "of" between "geometry" and "rotor blades ..."
- "Results": How was the performance variation quantified? Provide a figure for the performance gain per mission and/or per speed of flight.

Page 3:
- It is not clear enough, which flight regime was regarded (hover, forward flight, low/high speed, or both).
- Are the morphing concepts active or passive?
- Which frequencies or rotor harmonics were applied?
- Before the section named "Methods", a discussion of the state of the art is missing.

Page 4:
- After "... outboard region.": it is unclear where the flap is implemented.
- Para beginning with "In the torque-tube ...": Which range of twist angles was applied? Was it active or passive and which frequency was applied?
- Variables should be written in italics to identify them in the text. This holds for the whole text.

Page 6, Section "Optimization ...":
- The statement "... came at the cost of a high elastic twist" lets unclear which type of morphing is meant, variable chord or twist morphing or both.

Page 7, first line:
- Why is only the F_z component considered in the vibration criterion? F_x and F_y are not guaranteed to be small. There should at least be a statement in the results section that gives a qualitative assessment of their effect.

Page 8:
- "... data is available in literature (22)": This reference is not public, better cite the SABRE deliverable D1.1 which is public and contains all relevant data.
- Section "Rotor comprehensive analysis", line 2: what means "high resolution"? Quantify!

- The structural properties of the baseline blade are not provided. A description of changes to these structural changes is missing. How is the structural model composed? Which beam theory was applied and which spatial discretization was used? How was the structural model validated?
- Surrogate models: Description is missing.
- Data for the CFD model are missing/not referenced.
- The inflow model description is missing.

Page 9:
- The determination of the optimal hinge location is questionable: The data points in Fig. 7 do not allow to identify the minimum as precisely as mentioned in the text.
- The angle of attack for the data points in Fig. 7 are not provided.
- A definition of the Total Mission Objective is missing. How is it defined?
- Fig.7 should combine all results in one chart.

Page 10:
- Top of page: "... may not be fully trimmed ...": The untrimmed cases should not be used in Fig. 8. Otherwise the data points cannot be compared.
- Like in Fig. 7, the determination of the minimal hinge location is questionable.

Page 11:
- Table 4a: Explain why values for P% decrease while μ is increasing.
- Table 4b: Explain why values for P% remain constant while μ is increasing.
- Paragraph beginning "Figures 10a-c ...": The statements in this para are not supported by fig. 10a-c.
- Paragraph beginning "To summarize ...": Statement on elastic twist is insufficient, it should better be displayed in a figure.

Page 12 and 13:
- Plots are not readable without legend.

Page 14, first Para:
- F_z_4/rev at μ = 0.27 in Fig. 14 is conspicuously low especially when considering that quasi-static morphing mechanisms are involved (and not active blade morphing). Consequently, a description of underlying factors is deemed essential here and should be provided by the authors (much like the bevior of P is explained in the following para.
- Table 5a: What is $\Delta_\Theta = 1$ corresponding to?
- Tables 5a and 5b: Why is μ unequally spaced?

Page 15, Fig. 15:
- Add details (e.g. μ, flight case) to the caption.

Page 16:
- Abbreviations table covers only a part of the names of entities used in this text.

Is the work clearly and accurately presented and does it cite the current literature?
Partly

Is the study design appropriate and does the work have academic merit?
Partly

Are sufficient details of methods and analysis provided to allow replication by others?
No

If applicable, is the statistical analysis and its interpretation appropriate?
Not applicable

Are all the source data underlying the results available to ensure full reproducibility?
No source data required

Are the conclusions drawn adequately supported by the results?
No

Competing Interests: No competing interests were disclosed.

Reviewer Expertise: Rotorcraft aeromechanics, dynamics of rotating blades, aerodynamics of rotors

I confirm that I have read this submission and believe that I have an appropriate level of expertise to state that I do not consider it to be of an acceptable scientific standard, for reasons outlined above.

Author Response 25 May 2022

Rohin Majeti

Author responses in italics throughout.
General remarks:
The paper lacks a discussion of the state of the art in order to clearly identify where the authors' contribution is complementary to the publications in the literature list. This is an essential element of good practice in scientific writing. - *Updated state of the art. Done*

Detailed comments per page:
Page 1:

- First line: add "of" between "geometry" and "rotor blades ..."

Response: *Done*

- "Results": How was the performance variation quantified? Provide a figure for the performance gain per mission and/or per speed of flight.

Response: *Done*

Page 3:

- It is not clear enough, which flight regime was regarded (hover, forward flight, low/high speed, or both) – *a mission includes all the regimes.*
- Are the morphing concepts active or passive? - *passive*
- Which frequencies or rotor harmonics were applied? – *passive morphing*
- Before the section named "Methods", a discussion of the state of the art is missing. - *Done*

Response: *The introduction has been updated to address each of the above comments. As has*

been explained later in the article, the performance over a whole mission which includes a mix of flight regimes has been considered. The morphing concept is a passive, quasi-static one. The state-of-the-art discussion has been updated.

Page 4:

- After "... outboard region.": it is unclear where the flap is implemented. – *flap hinge is a variable determined by solving the optimization problem.*
- Para beginning with "In the torque-tube ...": Which range of twist angles was applied? Was it active or passive and which frequency was applied? – *passive morphing like in the case of chord morphing.*
- Variables should be written in italics to identify them in the text. This holds for the whole text. – *Done*

Response: *All the above comments have been addressed within the text. The flap hinge is a variable determined by solving the optimization problem. Torque-tube morphing is also a passive case like in the case of chord morphing; here the maximum twist angle is -16deg.*

Page 6, Section "Optimization ...":

- The statement "... came at the cost of a high elastic twist" lets unclear which type of morphing is meant, variable chord or twist morphing or both.

Response: *The statement is relevant for both the morphing concepts.*

Page 7, first line:

- Why is only the F_z component considered in the vibration criterion? F_x and F_y are not guaranteed to be small. There should at least be a statement in the results section that gives a qualitative assessment of their effects.

Response: *It is true that Fx and Fy components of the hub loads can also be significant. The Fz component contributes the most to the vibration in the fuselage and has been considered here to begin with. In follow up studies, the other components are also being considered.*

Page 8:

- "... data is available in literature (22)": This reference is not public, better cite the SABRE deliverable D1.1 which is public and contains all relevant data.- *Done*
- Section "Rotor comprehensive analysis", line 2: what means "high resolution"? Quantify! - *Done*
- The structural properties of the baseline blade are not provided. A description of changes to these structural changes is missing. How is the structural model composed? Which beam theory was applied and which spatial discretization was used? How was the structural model validated? – *Done*
- Surrogate models: Description is missing. - *Done*
- Data for the CFD model are missing/not referenced. - *Done*
- The inflow model description is missing. - *Done*

Response: *The text has been updated taking the above comments into consideration. It may be noted that the focus of the current paper is on the optimization problem and its solution methodology.*

Page 9:

- The determination of the optimal hinge location is questionable: The data points in Fig. 7 do not allow to identify the minimum as precisely as mentioned in the text.
- The angle of attack for the data points in Fig. 7 are not provided.
- A definition of the Total Mission Objective is missing. How is it defined? - *Done*
- Fig.7 should combine all results in one chart. – *Done*

Response: *Fig. 7 has been updated to include all results in one chart and the trimmed points were extended up to hinge locations of 0.68R by increasing the azimuthal resolution and minor adjustments in structural properties. The Total Mission Objective is defined in Eq. 5. The total mission objective has a decreasing trend towards outboard location of the morphing hinge until 0.64R after which it slightly increases. The angle of attack point was given with reference to Ref. 2 (section 3.4) where the example of hover condition was used to explain the possible cause of power reduction.*

Page 10:

- Top of page: "... may not be fully trimmed ...": The untrimmed cases should not be used in Fig. 8. Otherwise the data points cannot be compared. - *Done*
- Like in Fig. 7, the determination of the minimal hinge location is questionable. - *Done*

Response: *Using a combination of increased azimuthal resolution and minor adjustments in structural properties, a few of the earlier not-so-trimmed cases were improved and a few points up to hinge location of 0.68R added. The total mission objective has a decreasing trend towards outboard locations of the morphing hinge. This result serves to conclude that if the elastic twist of the blade and hub vibration levels are to be kept lower than or comparable to those of the baseline blade simultaneously, the extendable chord region has to be kept minimum which in turn reduces the potential for power reduction.*

Page 11:

- Table 4a: Explain why values for P% decrease while μ is increasing. - *Done*
- Table 4b: Explain why values for P% remain constant while μ is increasing. – *already given in the text*
- Paragraph beginning "Figures 10a-c ...": The statements in this para are not supported by fig. 10a-c.
- Paragraph beginning "To summarize ...": Statement on elastic twist is insufficient, it should better be displayed in a figure.

Response: *Text and figures have been updated taking above comments into consideration*

Page 12 and 13:

- Plots are not readable without legend. - *Done*

Response: *Plots have been updated to highlight the important data* Page 14, first Para:

- F_z_4/rev at μ = 0.27 in Fig. 14 is conspicuously low especially when considering that quasi-static morphing mechanisms are involved (and not active blade morphing). Consequently, a description of underlying factors is deemed essential here and should be provided by the authors (much like the bevior of P is explained in the following para.
- Table 5a: What is Δ_Θ = 1 corresponding to? - *-16deg*
- Tables 5a and 5b: Why is μ unequally spaced? – *Pre-defined search and rescue mission*

taken from refs 24, 25.

Response: *Text has been updated considering the above comments*

Page 15, Fig. 15:

- Add details (e.g. μ, flight case) to the caption.

Response: *As indicated in the caption, the flight case is that of hover (μ = 0.0).* Page 16:

- Abbreviations table covers only a part of the names of entities used in this text.

Response: *Done*

Competing Interests: No competing interests were disclosed.

Reviewer Report 18 October 2021

https://doi.org/10.21956/openreseurope.15151.r27794

© 2021 Shen W. This is an open access peer review report distributed under the terms of the Creative Commons Attribution License, which permits unrestricted use, distribution, and reproduction in any medium, provided the original work is properly cited.

?

Wen Zhong Shen
College of Electrical, Energy and Power Engineering, Yangzhou University, Yangzhou, China

The paper presents a design methodology for helicopter rotors with morphing blade. A chord morphing, a twist morphing, and a combined chord and twist morphing technique were used for the optimizations. Analyses on the designed results were made with respect to power, blade tip elastic torsion and hub vertical shear. It was found that the combined chord and twist morphing technique was spurious over the single chord or twist morphing technique. The paper is clearly written with sufficient detail and interest to read. The study was well designed and can be considered as a good example for designing other rotors than helicopter rotors. This reviewer has a number of questions or comments that can be considered to improve the paper.

1. Abstract: The authors mentioned “change the shape of blades in different regimes” in Background, while it is only “different missions” used in Methods. It needs some clarification whether the different regimes in the 3 missions were considered separately in the design.

2. Table 1, i2: The maximum chord extension seems a dimensional variable. If it is nondimensional, please indicate the reference chord. Same comment for the other non-dimensional parameters.

3. Equation 1: What is i? Mission or regime? Please specify.

4. Design constraints: “the rotor must be completely trimmed”. It would be good to indicate what parts of rotor were trimmed.

5. Page 7, Analysis: The notations in the inner and outer loops are confusing.

6. Page 8: “10 particles” and “20 particles” don’t seem a lot. Any justification?

7. Page 8: Can the chord length of the B105 rotor be provided?

8. Page 8, Left column, the last 3rd line: “as” to “is”.

9. Page 8: CFD needs to be given with more detail. Is it an unsteady code?

10. Page 8 “Based on this fresh CFD data, unsteady aerodynamic formulation”: How are the dynamic effects (such as dynamic stall) considered?

11. Some references are difficult to be accessed.

12. Results: The objective function was indicated for the inner loop. No information is given for the outer loop.

13. Figure 7: Why is the hinge location same for a complete mission as there are different regimes in a mission?

14. Page 11, Combined chord and twist morphing: Some information about the integration is useful to be given as there are inner and outer loops in both techniques.

15. Abbreviations: Some symbols are not listed. Please complete the list.

Is the work clearly and accurately presented and does it cite the current literature?
Yes

Is the study design appropriate and does the work have academic merit?
Yes

Are sufficient details of methods and analysis provided to allow replication by others?
Partly

If applicable, is the statistical analysis and its interpretation appropriate?
Not applicable

Are all the source data underlying the results available to ensure full reproducibility?
Partly

Are the conclusions drawn adequately supported by the results?
Yes

Competing Interests: No competing interests were disclosed.

I confirm that I have read this submission and believe that I have an appropriate level of expertise to confirm that it is of an acceptable scientific standard, however I have

significant reservations, as outlined above.

Author Response 25 May 2022

Rohin Majeti

Author responses in italics throughout.
Response to Reviewer 1 comments:

- Abstract: The authors mentioned “change the shape of blades in different regimes” in Background, while it is only “different missions” used in Methods. It needs some clarification whether the different regimes in the 3 missions were considered separately in the design.

Response: *Yes, as can be seen from the results later on, blade design (or blade shape) varies with flight regime in a mission. Within a flight regime, the blade shape remains constant. For example, in a mission, when the vehicle changes from one flight regime to another, say from hover to low-speed flight of 20m/s, the shape of the blade might have to change, say from 100% chord-extension to 50% chord-extension. During the entirety of hover, it retains the 100% chord-extension and during the entire 20m/s flight, it retains 50% chord-extension. The change in shape happens during the transition. The statement has been modified from “change the shape of blades in different regimes” to “change the shape of blades **between** different regimes” in a quasi-static manner.*

- Table 1, i2: The maximum chord extension seems a dimensional variable. If it is nondimensional, please indicate the reference chord. Same comment for the other non-dimensional parameters.

Response: *Table 1, i2 is a non-dimensional parameter given as a percentage of blade chord. The description has been updated in the table. The reference chord has been added to the blade parameters under the section ‘Analysis’..*

- Equation 1: What is i? Mission or regime? Please specify.

Response: *Equation 1 is the summation of the individual objectives f_1, f_2 and f_3. ‘i’ is the index for 1 to 3.*

- Design constraints: “the rotor must be completely trimmed”. It would be good to indicate what parts of rotor were trimmed.

Response: *Trim, here, refers to the set of control inputs to keep the rotor in equilibrium in a particular flight condition.*

- Page 7, Analysis: The notations in the inner and outer loops are confusing.

Response: *Text has been updated to make the notations clearer.*

- Page 8: “10 particles” and “20 particles” don’t seem a lot. Any justification?

Response: *Optimal swarm size is problem-dependent. A smooth search space will need fewer particles than a rough surface to locate optimal solutions. Swarm sizes of $n_s \in \epsilon$ [10, 30] have been shown to give optimal solutions for single objective problems. For the current problem, 10 and 20 particles were found to be adequate.*

- Page 8: Can the chord length of the B105 rotor be provided?

Response: *Chord length has been added to the reference blade description.*

- Page 8, Left column, the last 3rd line: “as” to “is”.

Response: *Done*

- Page 8: CFD needs to be given with more detail. Is it an unsteady code?

Response: *The DLR unstructured Navier-Stokes solver TAU was used for all computations with computations performed in viscous mode on a 2D airfoil section. New references have been given.*

- Page 8 “Based on this fresh CFD data, unsteady aerodynamic formulation”: How are the dynamic effects (such as dynamic stall) considered?

Response: *The unsteady aerodynamic formulation is based on the Leiss model. Further description has been added to this section in the article.,*

- Some references are difficult to be accessed. **--** Response: *References have been updated.*
- Results: The objective function was indicated for the inner loop. No information is given for the outer loop.

Response: *The outer loop objective function is given in Eq 5. It is the sum of the inner loop objective for each regime velocity multiplied by its weighting factor.*

- Figure 7: Why is the hinge location same for a complete mission as there are different regimes in a mission?

Response: *Physical construction of a moving hinge location is too complex and difficult to achieve. It has to be fixed for a particular blade (mission). So, in the algorithm, the hinge location is taken as the outer loop (mission) objective. Within the inner loop (regimes), the outer loop objective is kept constant.*

- Page 11, Combined chord and twist morphing: Some information about the integration is useful to be given as there are inner and outer loops in both techniques.

Response: *A short description has been added.*

- Abbreviations: Some symbols are not listed. Please complete the list.

Response: *Done*

Competing Interests: No competing interests were disclosed.